

---

**AURORA-B: An Evaluation Model  
for Boiling Water Reactors;  
Application to Control Rod Drop  
Accident (CRDA)**

ANP-10333Q1NP  
Revision 0

Responses to NRC  
Request for Additional Information

April 2017

AREVA Inc.

---

**Copyright 2017**

**AREVA Inc.  
All Rights Reserved**

AURORA-B: An Evaluation Model for Boiling  
Water Reactors; Application to Control Rod  
Drop Accident (CRDA)  
Responses to NRC  
Request for Additional Information

### Nature of Changes

Item	Section(s) or Page(s)	Description and Justification
1	All	Initial Issue

**Contents**

	<u>Page</u>
INTRODUCTION.....	1
RAI-1: .....	2
RAI-2: .....	8
RAI-3: .....	10
RAI-4: .....	16
RAI-5: .....	17
RAI-6: .....	25
RAI-7: .....	35
RAI-8: .....	41
RAI-9: .....	42
RAI-10: .....	44
RAI-11: .....	53
REFERENCES.....	55
APPENDIX A.....	56
APPENDIX B.....	59

### List of Tables

Table 1.1	Summary Impact of Surface Temperature weighting .....	3
Table 3.1	Impact on Enthalpy with Variation of Depletion Power .....	11
Table 3.2	Impact on Enthalpy with Variation of Depletion Power and Burnup .....	13
Table 5.1	End of Cycle Delayed Neutron Fraction.....	18
Table 5.2	BOC Candidate Rods .....	21
Table 5.3	PHE Candidate Rods.....	22
Table 5.4	EOC Candidate Rods .....	23
Table 6.1	Determination of Rod Failures for Assembly V17118 .....	28
Table 6.2	Determination of Rod Failures for Assembly V17134 .....	29
Table 6.3	V17118 Fission Gas Release Fraction Determination Reg. Guide 1.183 .....	30
Table 6.4	V17134 Fission Gas Release Fraction Determination Reg. Guide 1.183 .....	31
Table 6.5	V17118 Fission Gas Release Fraction Determination PNNL-18212 Rev 1.....	32
Table 6.6	V17134 Fission Gas Release Fraction Determination PNNL-18212 Rev 1.....	33
Table 6.7	Fission Gas Release Fractions For Assembly V17118 .....	34
Table 6.8	Fission Gas Release Fractions For Assembly V17134.....	34
Table 6.9	Equivalent Rod Failures.....	34
Table 7.1	Power Range Minimum CPR .....	40
Table 10.1	[  ] .....	45
Table 10.2	Uncertainty Parameters for CRDA Sample Problem Non- parametric Uncertainty Analyses .....	46

---

Table 10.3	Example of Ordered $\Delta H$ Results from Non-Parametric Statistical Process .....	48
Table 10.4	CRDA Test Case Results from Non-Parametric Statistical Process – ROD 118 Drop Location.....	50
Table 10.5	CRDA Test Case Results from Non-Parametric Statistical Process – ROD 121 Drop Location.....	51
Table 10.6	Maximum CRDA Enthalpy Rise Uncertainties .....	52
Table 11.1	Response to Change in Maximum Time Step Size.....	54

### List of Figures

Figure 1.1	Mid Range Burnup Temperature Rise .....	5
Figure 1.2	Higher Range Burnup Temperature Rise.....	5
Figure 1.3	Pellet Radial Power Distribution at Various Burnups .....	6
Figure 3.1	Peak Node Enthalpy Rise for Power Depletion Sensitivity.....	12
Figure 3.2	Example High Temperature Evaluation with Modified Power History.....	15
Figure 5.1	Establishing Evaluation Boundary .....	20
Figure 5.2	Example Evaluation Boundary .....	20
Figure 7.1	Starting Rod Pattern for PHE drop at 3875MW Rod 30-19.....	37
Figure 7.2	Adjusted Asymmetric Rod Pattern for PHE drop at 3875MW Rod 30-19 .....	38
Figure 7.3	Comparison of CPR Response with Asymmetric Initial Configuration .....	39
Figure 7.4	Power Range CPR Response CRDA .....	40
Figure 11.1	Trace of Enthalpy Rise with Different Maximum Time Steps .....	54

## INTRODUCTION

The AURORA-B CRDA LTR (Reference 1) was written to address interim criteria identified in SRP Section 4.2 Appendix B. Subsequent to the submittal of the CRDA LTR, Draft Regulatory Guide 1327 (Reference 3) has been proposed which has modified the criteria. Therefore, in addition to addressing the specific question posed, additional information has been included within the response indicating how the methodology could address criteria similar to that presented in DG-1327.

The original topical report was developed using the UDEC12 version of S-RELAP5. The information provided in this document has been developed using a new version of AURORA-B which contains updates to both S-RELAP5 and the MB2-K modules. Appendix A summarizes the justification for the code updates and describes the software change control process utilized by AREVA. As a result of the necessary code changes and other documentation issues found in the original topical report, AREVA will update select sections of ANP-10333P to ensure the final methodology is sufficiently captured by the approved version of the LTR. The updated topical report will be provided to the NRC in the released document ANP-10333PA, Revision 1.

## Potential Deviations

Two of the most important parameters used to determine if the interim acceptance criteria are met (fuel rod enthalpy and fuel temperature) are directly dependent on the magnitude of the power burst resulting from the CRDA. As a result, any potential deviation between the physical reality and the CRDA evaluation that may lead to a reduction in the limiting reactivity response in the CRDA analysis needs to be addressed. The NRC staff has identified some such potential deviations and determined that the following information is required in order to complete the evaluation.

### **RAI-1:**

*The primary mitigation mechanism for the CRDA event is the Doppler reactivity effect as the fuel temperature increases. The TR explains that this effect [*

*], which were set to maintain consistency with the steady state core simulator code (MICROBURN-B2). The CRDA event is a very fast transient that primarily consists of a fuel power/temperature response and its mitigation by negative reactivity due to Doppler feedback. As such, it would be expected to be more sensitive to the accuracy of the MB2-K treatment of the variation in the strength of the Doppler effect in the fuel rod due to variation in the fuel temperature. The TR provides results from a sensitivity study in section 8.7.3.11, but it is not clear how the study supports the selected weighting factors or the uncertainty associated with the pellet radial power distribution. Please provide a discussion of the technical basis supporting the weighting factors and the uncertainty selected for use with the CRDA analysis methodology, including the following:*

- a. changes in the radial fuel temperature distribution during the power excursion associated with the CRDA, and*
- b. the impact of fuel geometry changes due to irradiation (in particular, pellet growth and cracking) on the radial fuel temperature distribution.*

### AREVA Response RAI-1.:

The weighting factors were set consistent to those of the AURORA-B TR (ANP-10300) for consistency. The Doppler temperature is adequately reflected with the volume average [

] to the calculated enthalpy rise. [

] The Doppler effective temperature coefficient results from ANP-10333P (Table 8.19) have been recalculated with the latest code version and updated in Table B.11 of Appendix B. The data from Table B.11 has been recast in Table 1.1 to better show the impact of the surface weighting on the peak power, the prompt enthalpy, and total enthalpy.

**Table 1.1 Summary Impact of Surface Temperature weighting**

To better understand the basis for this behavior the following discussions are provided

- Changes in Radial Fuel Temperature Distribution
- Irradiation and Fuel Geometrical Changes
- Justification of Temperature Weighting and Uncertainty

### Changes in Radial Fuel Temperature Distribution

Changes in the radial fuel temperature distribution during the power excursion are illustrated in Figures 1.1 and 1.2 for rods with exposures of 22 MWd/MTU and 44 MWd/MTU respectively. During the initial power excursion the fuel pellet temperature increases rapidly at all radial nodes. (The center of the pellet is identified as node 1 and the surface is [

] The temperature in the outer regions of the fuel pellet begins to decrease shortly after the core power peaks as heat is transferred out of the pellet and to the coolant. However the inner portion of the fuel continues to rise in temperature. The pellet radial power profile varies with burnup due to changes in the radial isotopic distribution of fissile material with irradiation (because of Pu buildup at the pellet outer rim). Fresh UO<sub>2</sub> fuel pellets have a uniform radial isotopic distribution. Therefore, at beginning of life the power profile in the pellet in the radial direction only reflects the neutron thermal flux depression inside the pellet. As the fuel is irradiated there is a buildup of fissile plutonium isotopes from the resonance capture of neutrons in the U<sub>238</sub> and subsequent decay to fissile isotopes of plutonium. The majority of the neutron capture takes place at or near the pellet surface (self-shielding effect) resulting in burnup dependent power distribution as indicated in Figure 1.3. This radial power distribution is the combined effect of neutron thermal flux and fissile isotope distributions within the fuel pellet. These processes are accounted for in RODEX4 methodology (Reference 7).

The nodal ring [



**Figure 1.1 Mid Range Burnup Temperature Rise**



**Figure 1.2 Higher Range Burnup Temperature Rise**



**Figure 1.3 Pellet Radial Power Distribution at Various Burnups**

Irradiation and Fuel Geometrical Changes

During normal operation, the fuel pellet develops a number of cracks in the radial direction because of the parabolic temperature distribution, which creates tensile hoop stresses in the outer pellet region. These radial cracks are [

] The enhanced porosity occurs at the pellet outer rim and decreases the fuel thermal conductivity and is accounted for in RODEX4. Therefore, the impact of fuel geometry changes due to irradiation (such as pellet growth and cracking) are accounted for in the RODEX4 methodology and the mechanical model was accepted by the NRC (Reference 7, SER

Section 3.6). As such the fuel properties are defined with an approved methodology prior to the power excursion.

#### Justification of Temperature Weighting and Uncertainty

The increase in the prompt enthalpy with an increase in surface weighting is an [

] The prompt enthalpy is defined at the time of FWHM (full width half maximum) past the time of the peak power. An increase of the temperature surface weighting during the power ascension results in a higher effective temperature and more negative Doppler feedback. This reduces the peak power and [

] results in slight increase in the prompt enthalpy.

Following the rapid temperature rise, the surface temperature of the pellet begins to decrease as heat is conducted to the coolant. In this phase, the use of surface temperature weighting will have a [

] a conservative bias to the total enthalpy in that a cooler surface temperature is applied.

The use of the [ ] surface weighting provides a conservative bias for both prompt and total enthalpy rise. No credit is assumed for this conservative bias. The uncertainty reported was [

] profile in the fuel.

**RAI-2:**

*Page 8-24 of the TR discusses the technical basis for control rod modeling and its uncertainty. This discussion does not appear to address the fact that some control rods are designed with axial variations in neutron-absorbing material. Such variations may affect the reactivity insertion curve during a CRDA. Please provide a discussion of how axial variations in neutron-absorbing material used in the control rod blade will affect the reactivity insertion curve, including any limitations to the applicability of the recommended modeling approach and uncertainties.*

**AREVA Response RAI-2:**

Modern control blade designs may have varying axial cross section compositions (Paragraph 1 Section 2.2 Reference 4). The actual drop is performed with a single axial zoned control blade. More recent control blades with axially vary designs tend to have a slightly lower worth in the top node when hafnium is used. Also, newer blades may have a lower worth near the bottom with the removal of absorber material. The typical design criteria for new control blades demonstrate that the blade designs "meets all scram insertion criteria, reactivity control criteria, and CRDA" (Reference 5 Section 8).

Therefore utilization of a uniform axial blade composition with a worth [

] is consistent with blade design criteria. Even though some modern blades have a lower worth in the blade tip, the use of a higher worth blade tip increases the impact of the CRDA. In other words, more positive reactivity would be inserted when the dropped rod is modeled as a uniform axial blade as opposed to a blade which may contain some lower worth axial zones.

The uncertainty of the blade worth is accounted for within the methodology by utilizing a

[

] modeling uncertainty are included in the evaluation of the

methodology uncertainty shown in Table 8.20 of the CRDA LTR report. The methodology uncertainty is discussed further in the response to RAI-10.

The application of this methodology with respect to control blade designs is reflected in the methodology uncertainty. The control blade uncertainty used in the methodology has been selected consistent with current control rod designs, i.e. those designed to match worth with existing blade types. If new blade types are introduced in which the change in rod worth exceeds the blade uncertainty for the methodology, then adjustments are required by either choosing a blade type with a higher worth or by adjusting the blade uncertainty to assure that the range of blade worth's in the core remain bounded by the analysis.



in an increase in the total enthalpy rise. The impact of fission gas will only affect the [ ] occurs is essentially adiabatic.

There is no significant increase in gap conductivity with a decrease in the depletion power below nominal. This is to be expected since the release of fission gas during depletion at nominal conditions is already small, and a further reduction of this release due to reduced depletion power would have little effect. Therefore the total enthalpy rise increases for cases using a lower power level for the rod depletion which is consistent with the prompt enthalpy rise.

[ ]

**Table 3.1 Impact on Enthalpy with Variation of Depletion Power**

--



**Figure 3.1 Peak Node Enthalpy Rise for Power Depletion Sensitivity**

The steady state power distribution uncertainty and rod peaking factor were originally incorporated directly into the enthalpy uncertainty. However, the steady state power uncertainty is more appropriately reflected [

]

However, the steady state power uncertainty and the rod peaking factor will be conservatively retained in Table 8.20. (See RAI-10 for additional discussion of the uncertainty.)

Supplement to RAI-3 with respect to DG-1327

Subsequent to the submittal of the CRDA LTR, draft guidance (Reference 3) was published which changed the high temperature failure criteria. The proposed high temperature failure is decreased below that in SRP 4.2 and varies with the differential cladding pressure. Additional sensitivity cases were run to assess the adequacy of using the average rod power histories for the high temperature evaluation.

These additional sensitivity cases better illustrate the impact of the combined power level and burnup on the rod power histories. In the combined sensitivity evaluation, the rod power level was increased and decreased by both [

] also increased or

decreased. These results are provided in Table 3.2.

**Table 3.2 Impact on Enthalpy with Variation of Depletion Power and Burnup**



Both the combined results shown in Table 3.2 and the depletion power alone shown in Table 3.1 indicate that a large variation in the burnup history and depletion power has a very small impact on the enthalpy rise. However, the depletion power and burnup have a large impact on the internal rod pressure as a result of the amount of fission gas generated and the amount released from the pellet.

For evaluating the high temperature failure threshold, the rod internal pressure [ ] if the total enthalpy is greater than the minimum failure threshold. For illustration, the results from a cold case are used to demonstrate the application [ ] increase in rod depletion power and corresponding burnup. The enthalpy values determined from the nominal depletion results are tabulated against the differential pressure determined for both the nominal depletion and the high power/high burnup depletion histories. The transient fission gas release for rod pressurization is determined in accordance with Figure 6-1 of Reference 3, and [ ]

[ ] These results are shown in Figure 3.2 along with the proposed high temperature failure threshold from DG-1327. Fuel rods with a total enthalpy less than the minimum high temperature failure threshold (100 Cal/g in Figure 3.2) would not require application of the increased pressure. (The results in Figure 3.2 also indicate the small impact on fuel enthalpy with the variation in the fuel rod history.)



**Figure 3.2 Example High Temperature Evaluation with Modified Power History**

**RAI-4:**

*The sensitivity study documented in Section 8.7.2.3 for the core initial coolant temperature consists of a series of perturbations on the core initial coolant temperature. An increase in the core initial coolant temperature would result in a reduction in reactivity due to the corresponding increase in fuel temperature and the Doppler effect. If this was not compensated for in some other way (e.g., rod pattern adjustment), then the sensitivity studies may incorporate a less critical core as the starting point, which could reduce the severity of the prompt power pulse. Please provide a discussion of the effect of changes to the core initial coolant temperature on the initial reactivity of the core, and how they are captured by the sensitivity study.*

**AREVA Response RAI-4:**

The sensitivity study documented in Section 8.7.2.3 is not a true sensitivity with respect to coolant temperature alone. It is actually an evaluation of the temperature dependent reactivity compensation. This temperature dependent reactivity compensation decreases the event severity as the initial temperature is increased. Although using the lower temperature simulates a more reactive core, the AURORA-B system normalizes the eigenvalue to be critical. The fuel temperature and moderator conditions decrease the system reactivity as the temperature is increased. Therefore the use of the lower initial temperature as the initial condition for the drop will produce bounding results relative to the same rod drop configuration at a higher initial temperature. Although this lower temperature is used for the evaluation of the drop, [

] The

sensitivity results have been completed with the new code version and the results are included in Appendix B. The original conclusion remains supported.

### **Scenarios Selection**

Some of the details provided in the TR for the approach used to select CRDA scenarios for analysis do not include a justification that the approach is appropriate for its intended purpose. If the CRDA analysis is performed for scenarios that do not bound the worst case scenario, then a non-conservative result will be used to demonstrate that the acceptance criteria for the CRDA event are met. Therefore, the NRC has determined that additional information is needed to clarify how the selection process outlined in the TR to select the appropriate scenarios for analysis will bound all possible scenarios.

#### **RAI-5:**

*Page 7-8 states that the rod drop with the highest static rod worths at three exposures for the cycle are used in the CRDA evaluation, along with other candidate rods identified to evaluate the impact of the CRDA on fuel rods with high exposure and cladding content. The PCMI failure threshold is dependent on the hydrogen content in the cladding, so fuel with higher exposure may fail the acceptance criteria even if the prompt enthalpy rise is smaller than lower exposure fuel. In order to address this possibility, selection criteria are provided to guide the selection of additional rods as necessary. It is not clear how the proposed selection criteria will ensure that any potentially limiting rods will be identified for a broad range of possible cladding hydrogen contents, fuel types, and plant configurations. Please describe how the selection criteria will be effective in identifying suitable candidate rods for analysis that will ensure that the acceptance criteria are met, especially for fuel with cladding hydrogen content in the range where the failure threshold rapidly decreases (75 to 150 ppm).*

#### **AREVA Response RAI-5:**

The [

Table 5.1 shows actual end of cycle core average delayed neutron fractions for several recent AREVA fuel reloads. These results include both 18 and 24 month cycle lengths and a range of core sizes from 408 to 800 assemblies.

**Table 5.1 End of Cycle Delayed Neutron Fraction**



The criteria and evaluation process are revised to account for broad range of potential failure thresholds and core loading strategies. This revised selection criteria is now independent of the actual form of the failure threshold criteria and core loading strategy.

The selection will be based on [

] provides a method to assure that an intermediate failure threshold would not be exceeded. EOC evaluations will utilize the minimum failure threshold at that condition [ ]

During the initial application for a given plant group or fuel loading type, rod drops for a range of rod worths greater than [

] The results of this initial evaluation are

[

] The establishment of the evaluation boundary is illustrated in Figure 5.1.

Candidate control rod drops and the minimum failure threshold are tabulated and compared with the evaluation boundary. To apply the evaluation boundary, the y-axis is changed from [ ] as shown in Figure 5.2. Candidate rods for which the minimum failure threshold [

] since the drop will not challenge the failure threshold.

However, a drop with a minimum failure threshold [

] requires additional evaluation.



**Figure 5.1 Establishing Evaluation Boundary**



**Figure 5.2 Example Evaluation Boundary**

Following is an example application to demonstrate this process.

As discussed previously, the evaluation [ ]

application. The rod drops with worth values greater than [ ]

[ ] at BOC, PHE (peak hot excess) reactivity, and EOC. The first tabulation at BOC is given in Table 5.2. In this example the failure thresholds around the rods are [ ]

[ ] only the highest worth drop is evaluated. Since there are no failures the dose limits are not exceeded for the BOC rod drops using failure criteria determined for the [ ]

[ ]

**Table 5.2 BOC Candidate Rods**

[ ]
-----

The tabulation at PHE is given in Table 5.3. Only a few drops were found with worth values greater than [ ] and no candidate rods were to the [ ]

[ ] Therefore, only the highest worth rod is evaluated. Since the maximum enthalpy rise is less than the [ ]

[ ] no additional evaluation of the PHE rods is required [ ]

**Table 5.3 PHE Candidate Rods**



The tabulation at EOC candidate rods is given in Table 5.4. Several rod worth values are greater than [ ] This is primarily due to the gadolinium burnout in this cycle. The minimum failure threshold is similar for several rods. Evaluation of the highest worth rod is completed for [ ]

[ ] Rods 12, 87, 174, 14, and 102 are one row in from the edge. Rods 83, 155, and 37 have similar fuel loading and failure thresholds. Although the maximum fuel enthalpy exceeds the [ ]

the final evaluation is made by comparing the individual enthalpy rise for each fuel rod to its specific failure threshold. If fuel rod failures are determined the dose consequences are then evaluated.

**Table 5.4 EOC Candidate Rods**

In the above example, the fuel enthalpy rise for BOC and PHE were less than the failure criteria [ ] However, if the assembly fuel enthalpy rise results in fuel failures based on the [

] but are exceeded at the [

]

[

]

It is anticipated that with the application of the methodology additional data results can be tabulated and that a generic evaluation boundary curve may be established.

The actual selection process is presented in the following steps:



(See the response for RAI-9 for discussion of step 5.)

**RAI-6:**

*Section 7.6 discusses the approach used to determine rod enthalpy increases for individual fuel rods, which is then used to determine how many rods will experience PCMI failure for fission gas inventory release purposes. The text is not clear regarding how the [*

*why this assumption [ ] Please describe  
] would be  
expected to yield bounding results of fission gas inventory releases for all possible fuel lattices, including those with strong poisons that have not yet fully burned out or those that have experienced strongly asymmetric operating conditions (e.g., adjacent control rod insertion).*

**AREVA Response RAI-6:**

This approach has been revised to address the entire history of the fuel assembly. The [

*] individual pin enthalpies using the peak and average enthalpy rise at each axial level of each assembly. The average is increased [ by 3% (multiplied by 1.03) to address the rod peaking factor uncertainty of 1.48 ] discussed in Section 8.7.3.12 of the CRDA LTR. The following equation will replace Equation 3 within Section 7.6 of the CRDA LTR.*

[

]

A fuel pin is determined to fail if it exceeds its failure threshold at any axial level.

$$PINF_i = \begin{cases} 1 & \text{If } (\Delta h_{i,k} > \Delta hf_{i,k}) \text{ for all } k \\ 0 & \end{cases}$$

Where  $PINF_i$  is a fuel rod failure flag

$\Delta h_{i,k}$  is the enthalpy rise in fuel rod  $i$  at axial level  $k$  (with uncertainty multiplier)

$\Delta hf_{i,k}$  is the enthalpy failure threshold for fuel rod  $i$  at axial level  $k$

The total number of fuel rods failed (NFAIL) in an assembly is then the summation of the individual fuel rod failure flags.

$$NFAIL = \sum_{L=1}^{n_{pin}} PINF_i$$

The enthalpy that is used for the determination of the transient fission gas release (TFGR) for evaluation of dose consequence is determined for each axial node as the

[

]

Sections 7.6 and 9.5 of the CRDA LTR will be revised to reflect this change. The example provided in Section 9.5 was reevaluated using [

] The tabulation of fuel rod failures for two assemblies are provided in Table 6.1 and 6.2. Tables 6.3 through 6.6 contain the average release

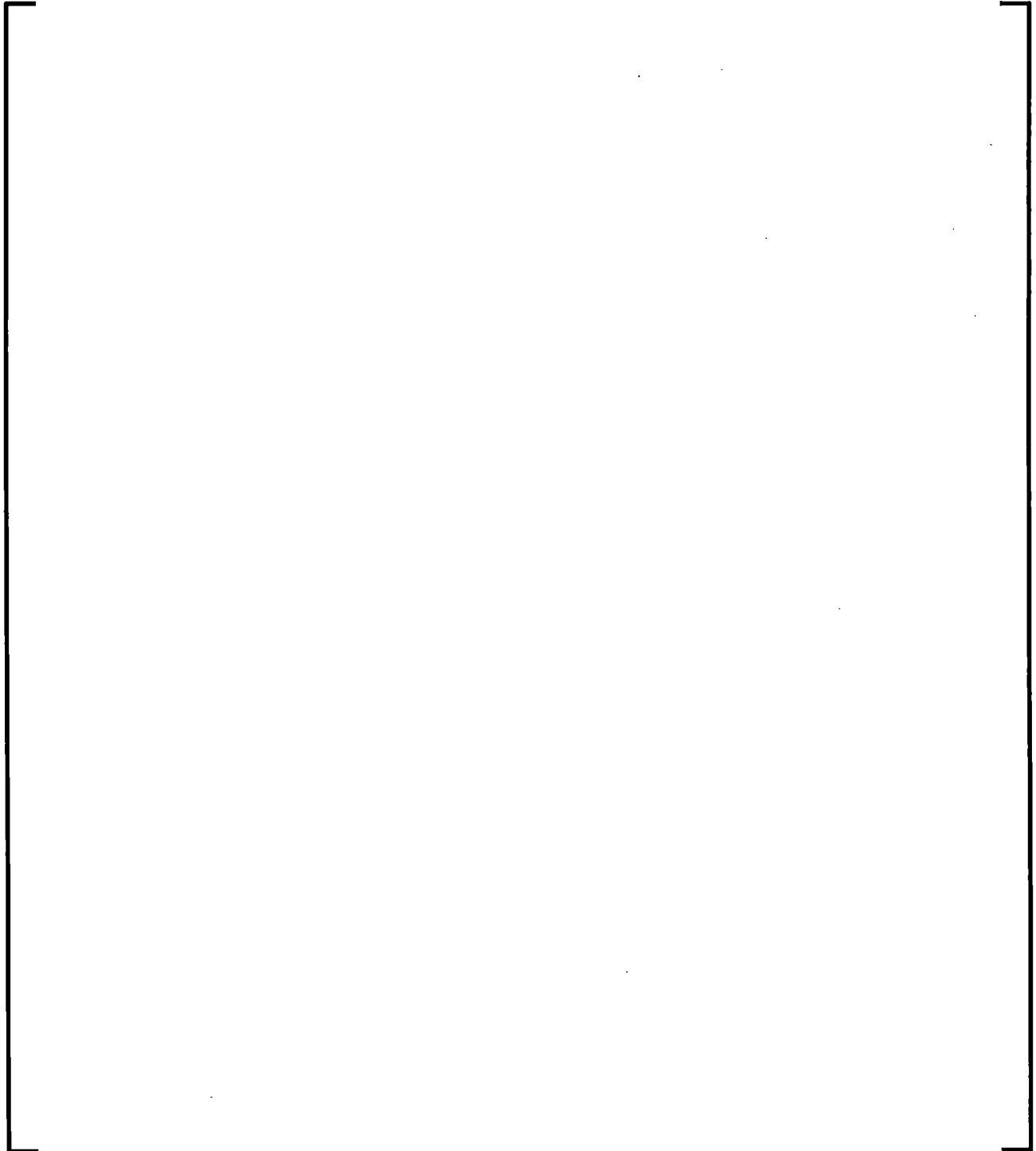
fractions for two assemblies using SRP-4.2 release fractions and PNNL-18212 R1 release fractions.

Table 6.7 and 6.8 contain the [

] as shown in Table 6.9.

Changes in the final fission gas release formulation for evaluation of dose consequences, such as those proposed in DG-1327, would be handled in a manner consistent with the process demonstrated in the example problem.

**Table 6.1 Determination of Rod Failures for Assembly V17118**

A large, empty rectangular frame with a thin black border, centered on the page. It is intended to contain the data for Table 6.1, but the content is missing from this scan.

**Table 6.2 Determination of Rod Failures for Assembly V17134**

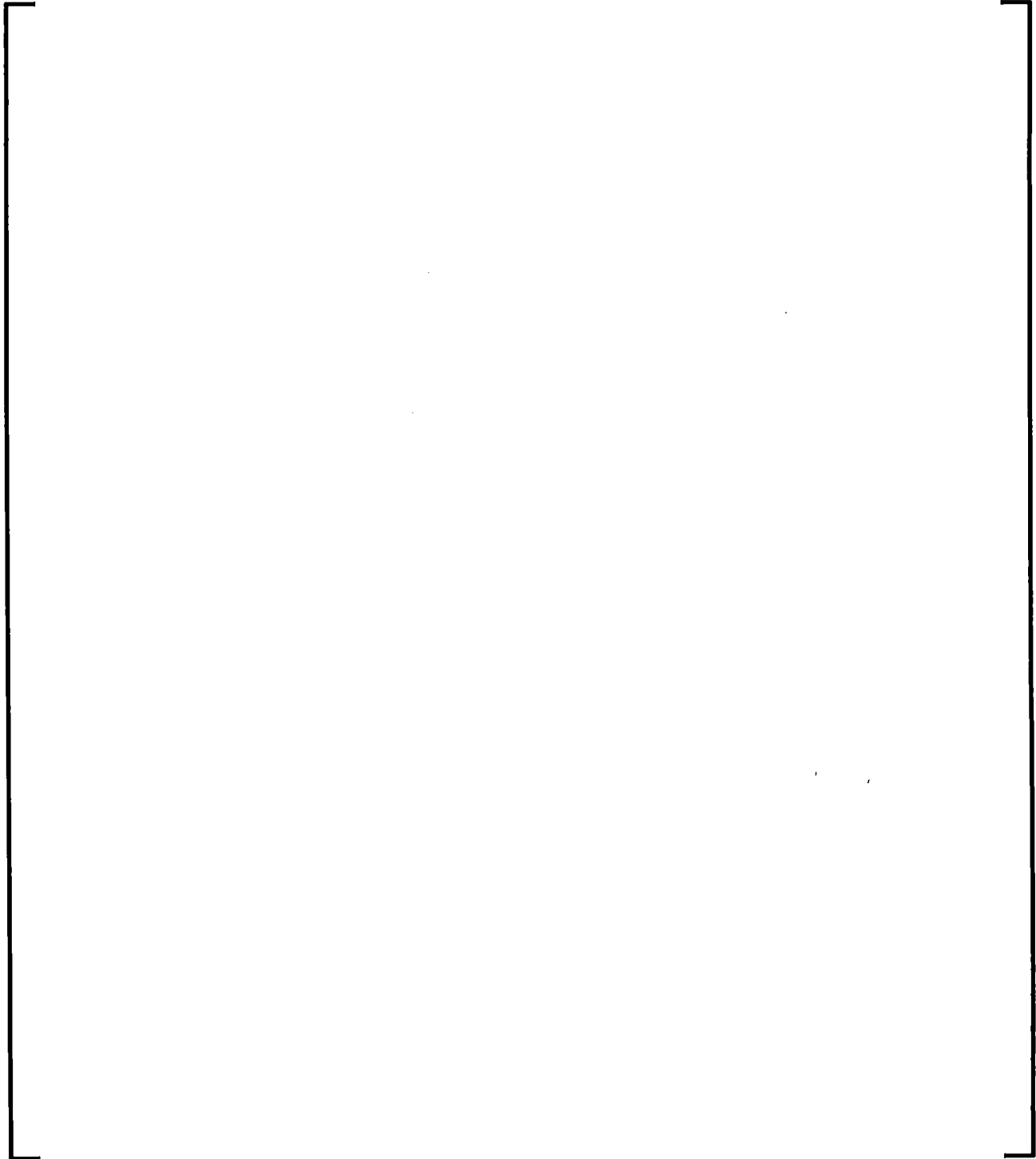


**Table 6.3 V17118 Fission Gas Release Fraction Determination Reg. Guide 1.183**

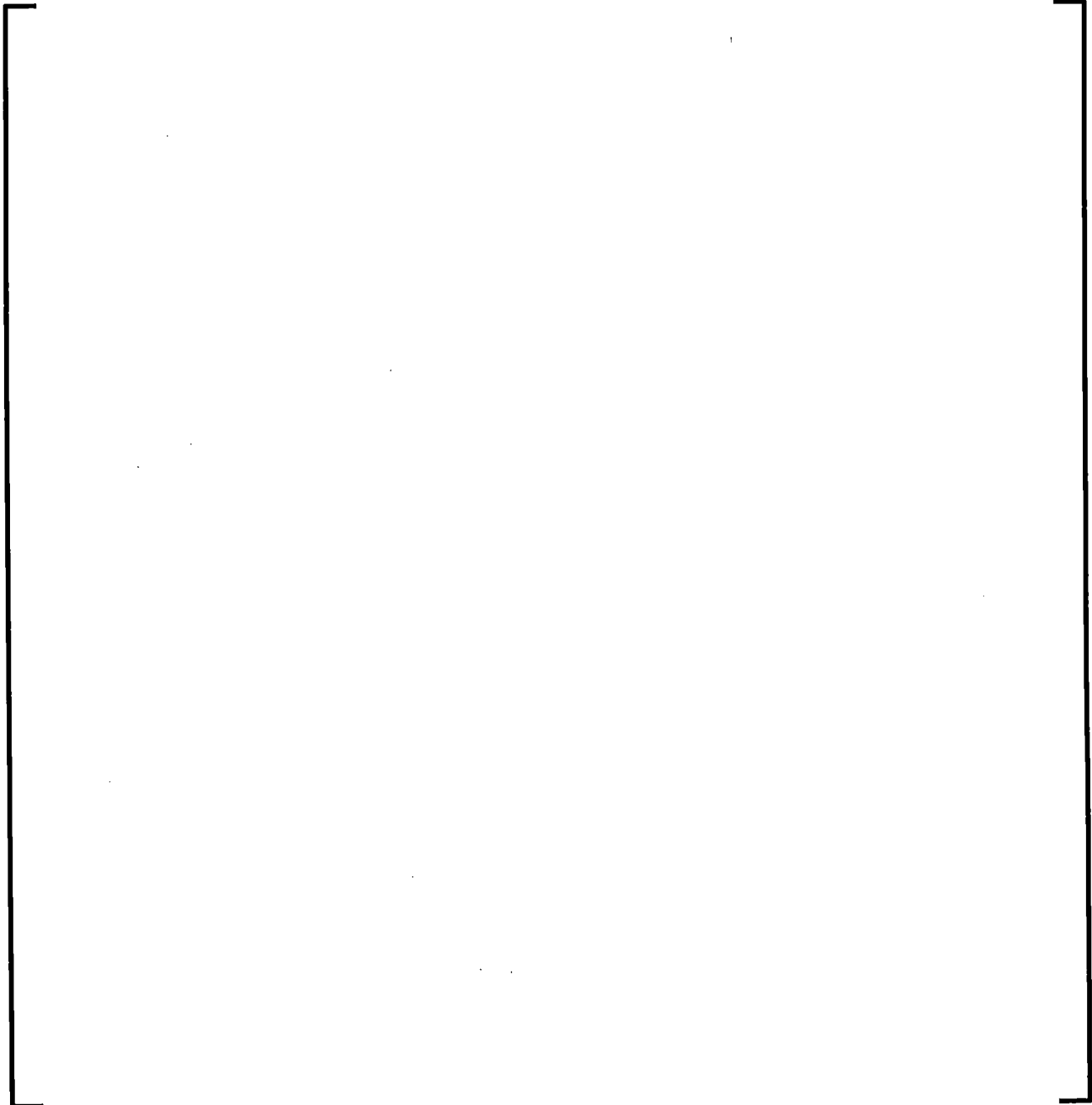


**Table 6.4 V17134 Fission Gas Release Fraction Determination Reg. Guide 1.183**

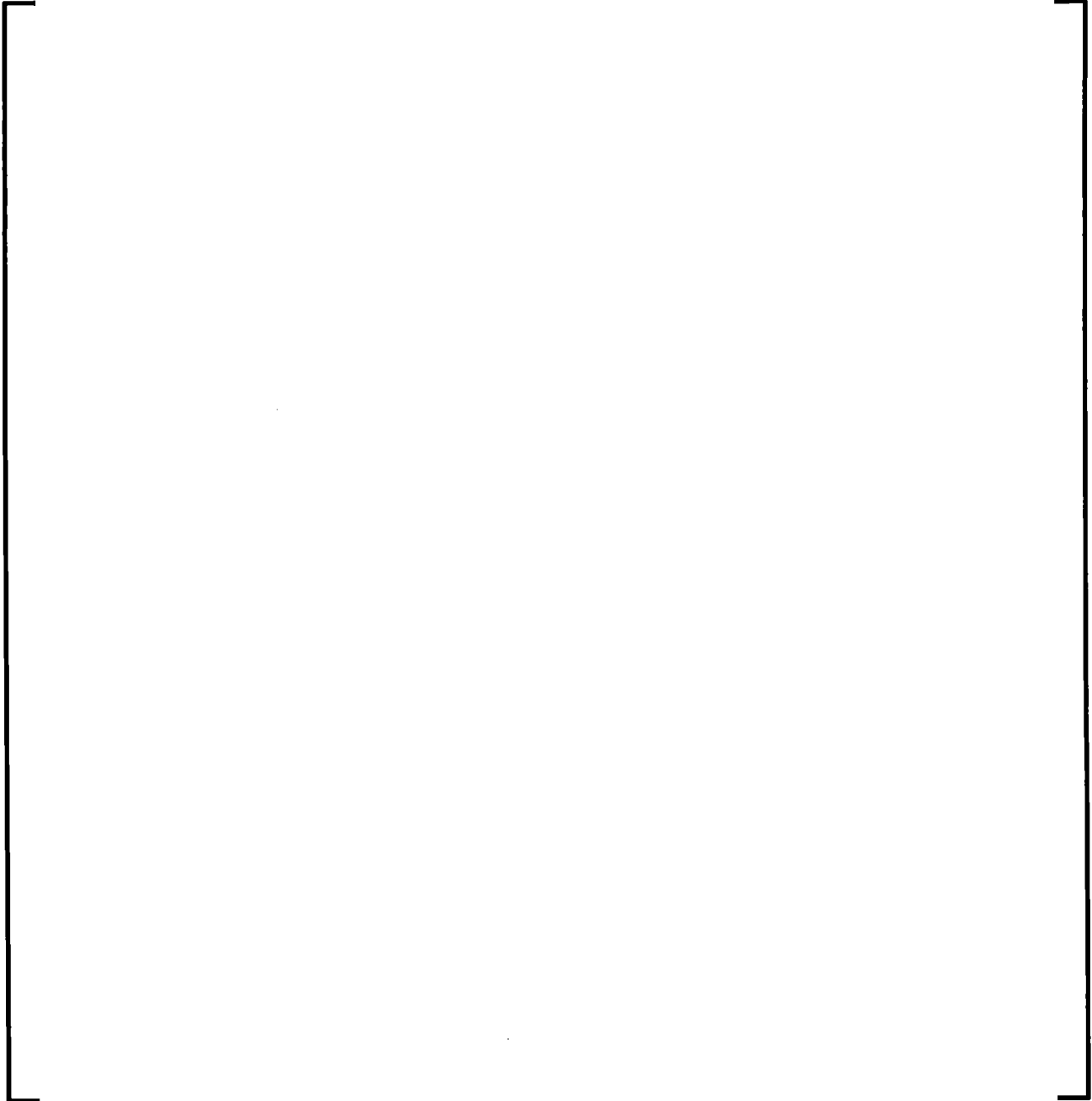


**Table 6.5 V17118 Fission Gas Release Fraction Determination PNNL-18212 Rev 1**

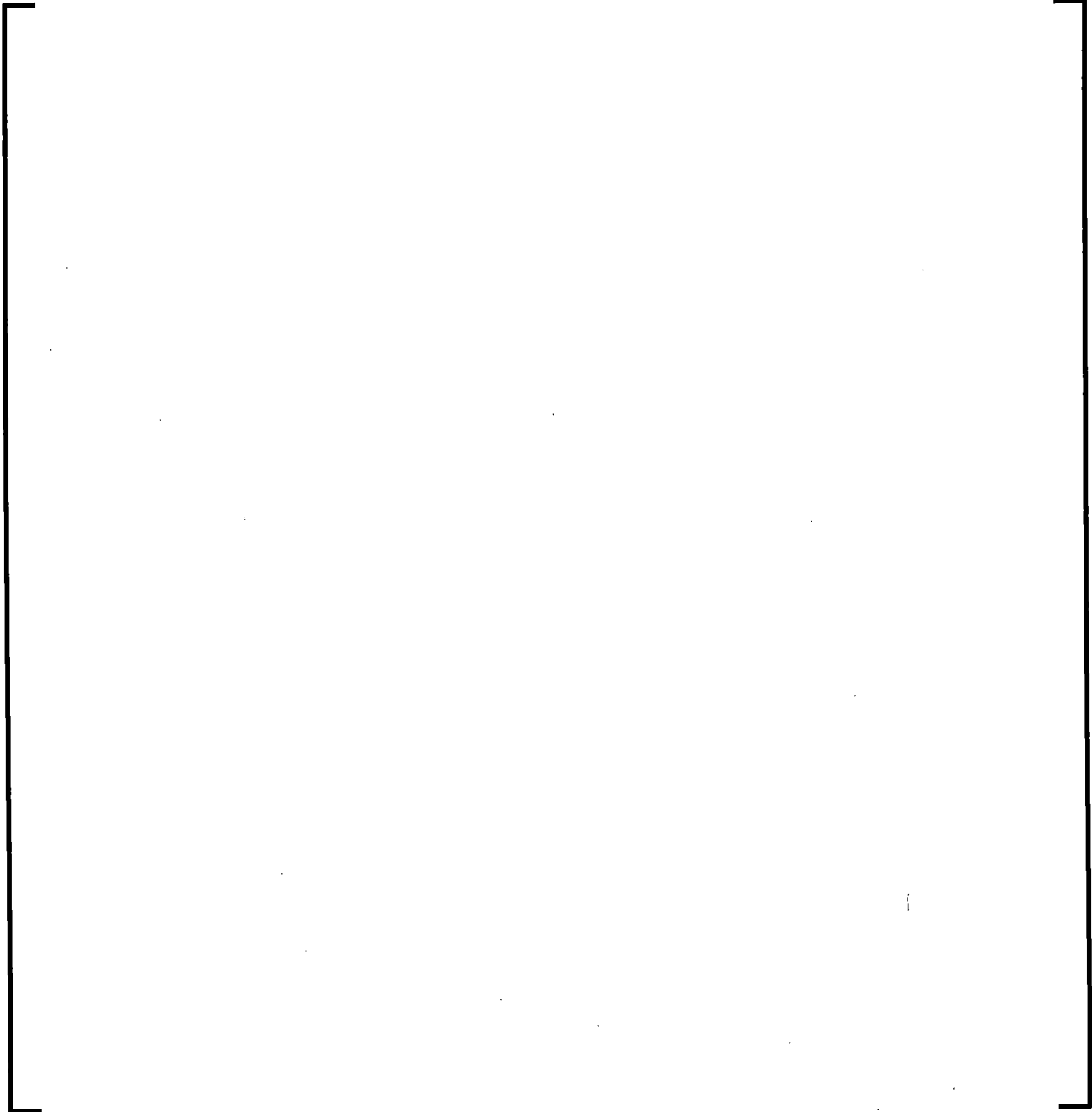


**Table 6.6 V17134 Fission Gas Release Fraction Determination PNNL-18212 Rev 1**

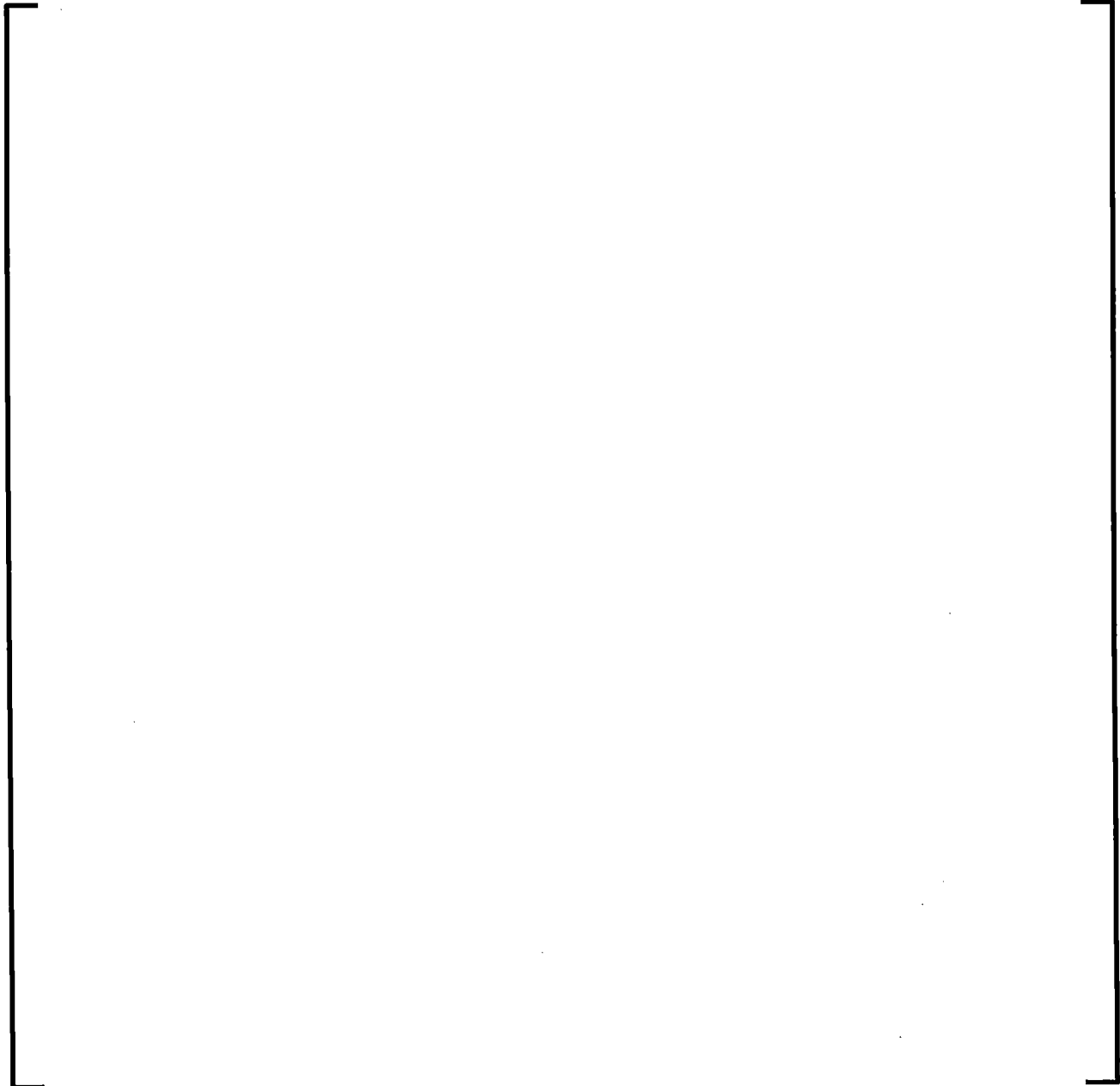


**Table 6.7 Fission Gas Release Fractions For Assembly V17118**



**Table 6.8 Fission Gas Release Fractions For Assembly V17134**

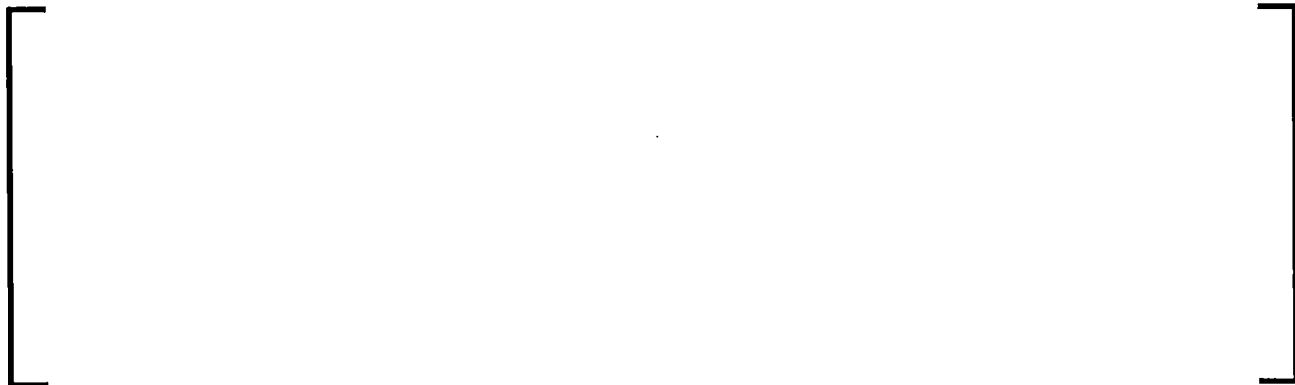


**Table 6.9 Equivalent Rod Failures**



**RAI-7:**

*Section 7.7 describes the evaluation of the CRDA event for at-power conditions using the critical power ratio (CPR). The proposed approach seems sufficient for typical analyses, but it is not clear how broad the generic applicability of the analysis is. Based on the discussion in the TR, it appears that the [*

*]. If that is true, please describe how unusual operating conditions may affect this determination, such as insertion of suppression rods which result in a radial asymmetry in the core power distribution.*

**AREVA Response RAI-7:**

The evaluation of MCPR response in Section 7.7 of the LTR is [

    ] The negative reactivity from the generation of significant or increased voiding dampens the impact of the BWR CRDA when the event occurs "at-power" conditions as opposed to the unvoided startup conditions. The power pulse in the power range (Figure 7.10 of the CRDA LTR) shows a very broad pulse with limited power increase. The results provided on Page 7-26 of the CRDA LTR as well as the results provided later in this response demonstrate that the CPR [

    ] These results and conclusions are consistent with the reduced impact for power range rod drop as discussed in Reference 9 page 3-2. The characteristic behavior of the BWR with respect to void reactivity is independent of plant type.

**Impact of Asymmetric Operation**

An evaluation has been performed to address the question of the impact of asymmetric operation, such as may be encountered with the insertion of suppression rods. In the process of evaluating the impact of the asymmetric power distribution it was discovered

that some of the initial cases reported in Table 7.7 and Figure 7.11 of the CRDA LTR were incorrect due to an input error. This error has been documented in AREVAs corrective action program and the corrected results are provided later in this response. The asymmetric operation evaluation results are compared to these corrected results.

The possibility of unusual operating conditions such as stuck control rods or insertion of suppression rods could result in a radial power asymmetry in the core. It is anticipated that in such circumstances that the plant would be operated in conditions as close to the nominal cycle licensing basis as possible. To address asymmetric operation, an additional evaluation was performed by inserting suppression rods and then simulating a rod drop. The initial pattern and the modified rod pattern with asymmetrical operation are given in the Figures 7.1 and 7.2, respectively. It is noted that to maintain the eigenvalue additional modifications were made to the control rod pattern.



**Figure 7.1 Starting Rod Pattern for PHE drop at 3875MW Rod 30-19**



**Figure 7.2 Adjusted Asymmetric Rod Pattern for PHE  
drop at 3875MW Rod 30-19**

Rod 30-19 was dropped and the resulting MCPR was evaluated. A comparison of the MCPR between the two rod drops is provided in Figure 7.3. [

] The change in void reactivity feedback for the BWR is small since the core average void would be similar between symmetric and asymmetric power distributions. This void reactivity feedback limits the severity of the rod drop when operating in the power range. Therefore there is only a small impact on the CPR change due to the suppression rods.



**Figure 7.3 Comparison of CPR Response with Asymmetric Initial Configuration**

Supplemental Information Regarding Identified Calculation Error

[

As such the conclusion drawn from the original CRDA LTR results is not challenged by the corrected results and remains valid.

In the corrected evaluation, the rod selected for BOC was changed to a more conservative rod drop which resulted in a decrease in the BOC CPR at 88% power.

The selection of the more conservative rod for BOC conditions and [

] in the CRDA LTR.

Table 7-7 and Figure 7.11 of the CRDA LTR will be replaced with the corrected results provided in Table 7.1 and Figure 7.4 of this response.

**Table 7.1 Power Range Minimum CPR**



**Figure 7.4 Power Range CPR Response CRDA**

**RAI-8:**

*The TR does not appear to discuss the applicability of this methodology to mixed cores. Please describe any limitations or changes necessary to account for cores with non-AREVA fuel, including evaluation parameters not directly involved in the CRDA calculation such as the cladding hydrogen content.*

**AREVA Response RAI-8:**

The neutronic and transient modeling for the CRDA will be completed with the same methodology regardless of fuel type. The modeling will explicitly consider geometric differences in fuel designs present in mixed core applications. The fuel mechanical properties of UO<sub>2</sub> pellets and zircaloy cladding are modeled with the RODEX-4 code for each fuel type according to the respective fuel mechanical properties. The sensitivity studies show that there is little impact on the actual event based on the variation of the rod thermal mechanical properties. Therefore, the establishment of the rod thermal mechanical properties with the RODEX4 code is appropriate. The database used to develop the AREVA hydrogen uptake model includes recrystallized (RXA) cladding typically used in non-AREVA fuel. It is anticipated that the AREVA hydrogen uptake model will be used for all fuel types. However, hydrogen uptake models designated as acceptable by the NRC such as those in Reference 6 may be used for other vendor cladding.

With respect to the evaluation of MCPR for mixed core configurations, AREVA utilizes an NRC-approved process (Reference 8) for developing additive constants (correlation coefficients) to apply the AREVA CPR correlations to the non-AREVA fuel types.

Sensitivity studies were performed on various input parameters for the CRDA calculation. In some cases, these studies were used to support use of a bounding value for the CRDA analysis. In other cases, the study results were used to support a value for the uncertainty in the enthalpy rise. These studies and their results are used to provide reasonable assurance that the results of the CRDA analysis will bound real-world conditions. The NRC identified some cases where the sensitivity study approach or the conclusions did not clearly support the intended purpose, so further information is necessary.

**RAI-9:**

*A number of the conclusions derived from the sensitivity studies do not appear to be supported by the actual results from the calculations performed for the studies. For example, section 8.7.2.5 discusses the sensitivity of the CRDA analysis results to the initial core flow. The text states that the prompt enthalpy rise decreases as the initial core flow increases, while the total enthalpy increases as the initial core flow increases. This is used to support the use of a minimum core flow as a bounding value for determining the prompt enthalpy rise. However, no clear recommendation is given for evaluation of the total enthalpy, and the sensitivity studies show that the limiting value for the prompt enthalpy rise was calculated for an initial core flow just above the recommended minimum value. Please provide further clarification for the behavior of the prompt enthalpy rise as a result of variations in the initial core flow, and provide guidance on the appropriate initial core flow to use when evaluating the total enthalpy.*

**AREVA Response RAI-9:**

The sensitivity studies in Section 8.7.2 and 8.7.3 of the CRDA LTR have been evaluated with the enhanced convergence methodology and are included in Appendix B. The revised sensitivity results for the initial core flow (Table B.3) indicate between [

] Although the total enthalpy increases with the initial core flow, to achieve a higher core flow would require the addition of heat from recirculation pumps, decay heat, or actual power generation. The results of the sensitivity with respect to the initial temperature show that an increase in initial coolant temperature significantly

reduces the enthalpy rise. Therefore use of the lower flow temperature conditions should bound the results for the high temperature evaluation based on total enthalpy. To ensure this, an additional step has been added to the evaluation process (see RAI-6 response) to confirm the results from the low flow evaluation bound that of the high flow condition.

The additional step assures that the total enthalpy is evaluated at the initial flow conditions which results in the highest total enthalpy.

**RAI-10:**

*Section 8.7.4 states [*

*]* Please provide  
*a justification for the appropriateness of the statistical approach used.*

**AREVA Response RAI-10:**

[

**Table 10.1 [**

**]**

[

]

[

]

**Table 10.2 Uncertainty Parameters for CRDA Sample  
Problem Non-parametric Uncertainty Analyses**



With the exception of parameter rod worth, the sampling ranges used for all of the parameters in the above table are the same as those used for the AOO methodology, as shown Section RAI-49b of the RAI responses for the AOO methodology (ANP-10300Q2P).

Parameter rod worth is a new sampling parameter. Since rod worth cannot be sampled directly through [

]

Lattice calculations were performed to generate modified cross sections which

represented an [

]

An example of ordered prompt and total  $\Delta H$  results for test case ROD121 is seen in Table 10.3. A sample ensemble [

]

[

]

**Table 10.3 Example of Ordered  $\Delta H$  Results from  
Non-Parametric Statistical Process**

[

]

[

]

[

]

Two of the parameters originally included in Table 8.20 of the CRDA LTR were not included in this evaluation; the power distribution and rod peaking factors. [

] Therefore they are omitted from this evaluation.

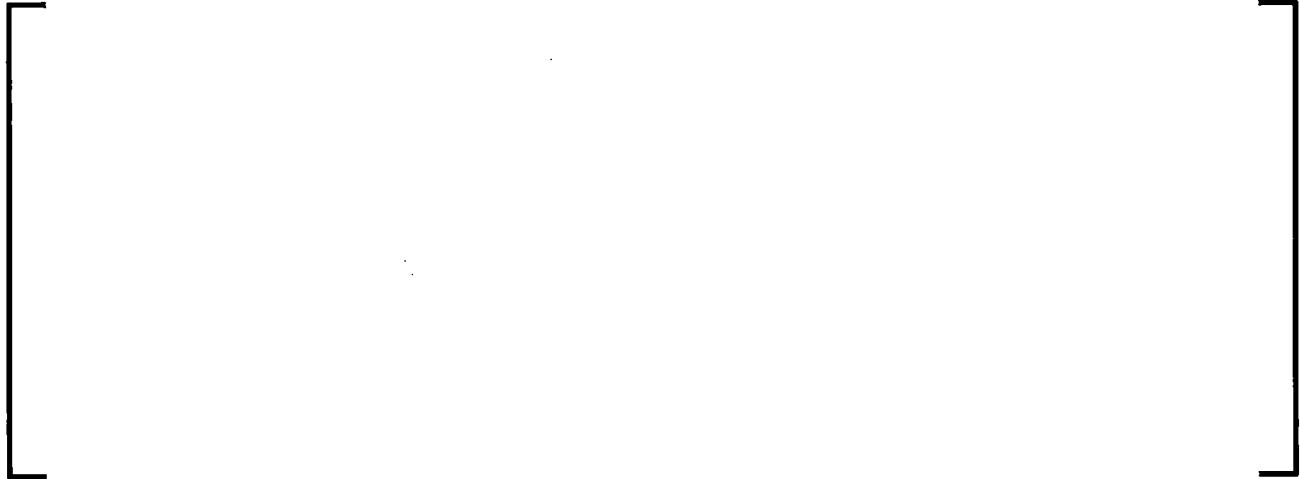
**Table 10.4 CRDA Test Case Results from Non-Parametric  
Statistical Process – ROD 118 Drop Location**

A large, empty rectangular frame with a thin black border, centered on the page. It is intended to contain the data for Table 10.4, but the content is missing.

**Table 10.5 CRDA Test Case Results from Non-Parametric  
Statistical Process – ROD 121 Drop Location**

A large, empty rectangular frame with a thin black border, centered on the page. It appears to be a placeholder for a table that is not present in this version of the document.

**Table 10.6 Maximum CRDA Enthalpy Rise Uncertainties**

A large, empty rectangular frame with a thin black border, centered on the page. It is intended to contain the data for Table 10.6, but the content is missing.

**RAI-11:**

*The TR recommends a different time step size for some CRDA evaluations due to the nature of the transient. Sensitivity studies were performed to determine the impact of any further changes in time step size. However, it is not clear how the specific value recommended in the TR was determined. The documentation of the sensitivity studies only discusses calculations performed at a different time step size. Please clarify if the discussion on the time step sensitivity in Section 8.7.1 was intended to characterize the sensitivity study as showing that a further change in time step size beyond the recommendation in Table 7.5 would not yield a significant change in calculated enthalpy. If the NRC staff interpretation is in error, please provide sufficient information to enable an understanding of how the sensitivity study relates to the final recommendation on time step sizes.*

**AREVA Response RAI-11:**

Sensitivity studies were performed with respect to the maximum time step size. The actual numerical results of the study, provided in Table 11.1 do not lead to a straight forward conclusion. For this case, some of the larger maximum time steps actually lead to higher deposited enthalpies and the prompt and total enthalpy rise did not always trend in the same direction.

The time trace plots (Figure 11.1) show that the results converge as the time step size is decreased. Based on the comparison traces the time steps sizes of Table 7.5 of the CRDA LTR are specified.

**Table 11.1 Response to Change in Maximum Time Step Size**

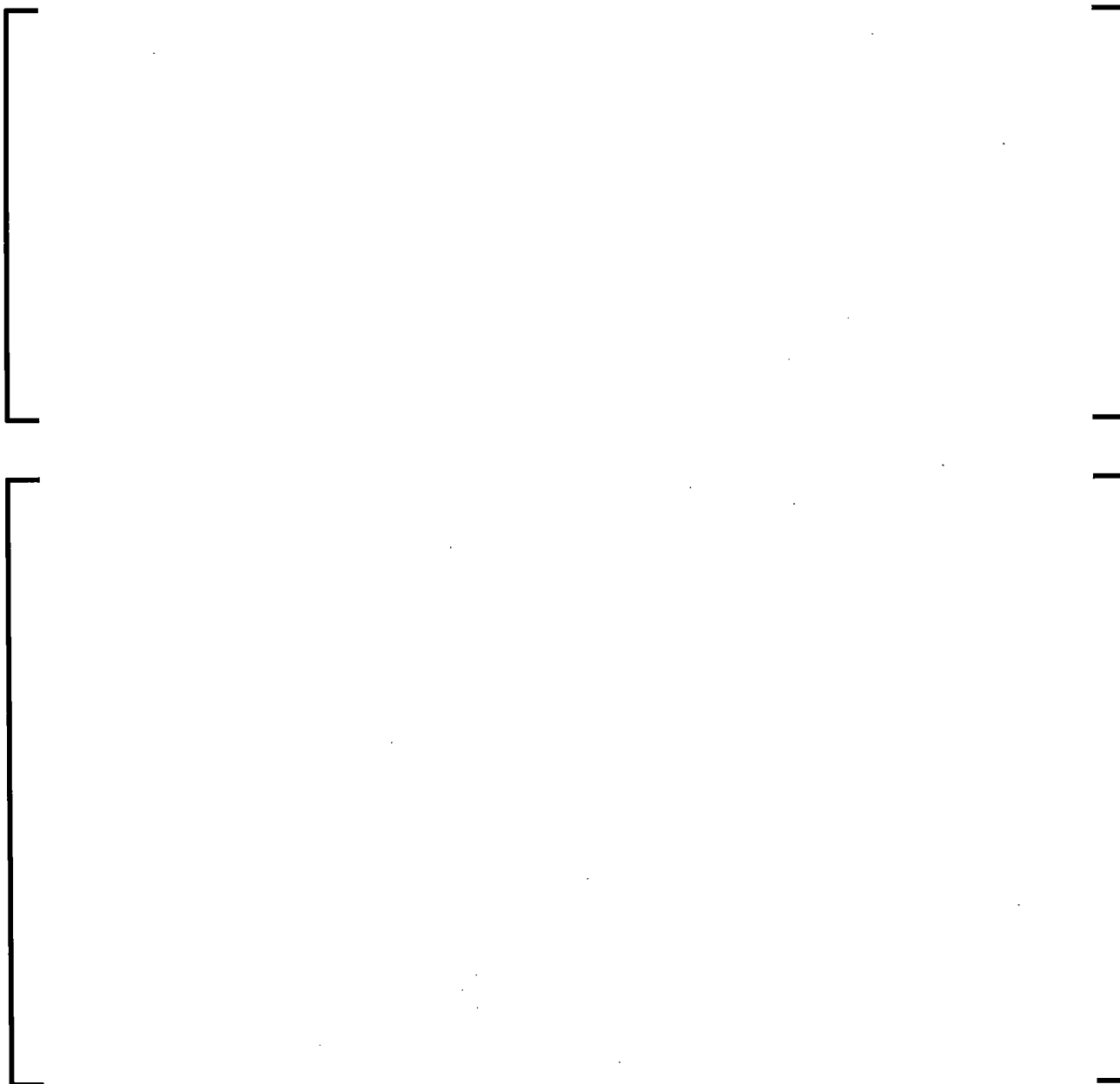


**Figure 11.1 Trace of Enthalpy Rise with Different Maximum Time Steps**

## REFERENCES

1. ANP-10333P Revision 0, "AURORA-B: An Evaluation Model for Boiling Water Reactors; Application to Control Rod Drop Accident (CRDA)," AREVA, Inc., March 2014.
2. ANP-10300P Revision 0, "AURORA-B: An Evaluation Model for Boiling Water Reactors; Application to Transient and Accident Scenarios," AREVA NP, Inc., December 2009.
3. US NRC Draft Regulatory Guide DG-1327, *Pressurized Water Reactor Control Rod Ejection and Boiling Water Reactor Control Rod Drop Accidents*, November 2016. (NRC ADAMS ML16124A200)
4. WCAP-16182-NP Revision 3, *Westinghouse BWR Control Rod CR 99 Licensing Report – Update to Mechanical Design Limits*, August 2016 (NRC ADAMS ML16235A108)
5. NEDO-33284-A Revision 2, *Marathon-5S Control Rod Assembly*, October 2009 (NRC ADAMS ML092950284)
6. Memorandum from Paul M. Clifford (NRC) to Timothy J. McGinty (NRC) "Acceptable Fuel Cladding Hydrogen Uptake Models," May 13, 2015. (NRC ADAMS ML15133A306)
7. BAW-10247PA, Revision 0, "Realistic Thermal-Mechanical Fuel Rod Methodology for Boiling Water Reactors," AREVA NP, February 2008.
8. EMF-2245(P)(A), Revision 0, "Application of Siemens Power Corporation's Critical Power Correlations to Co-Resident Fuel," Siemens Power Corporation, August 2000.
9. NEDO-10527, *ROD DROP ACCIDENT ANALYSIS FOR LARGE BOILING WATER REACTORS*. Class I. General Electric: San Jose, CA. (NRC ADAMS ML010870249)

## APPENDIX A

### CODE ISSUES AND METHODOLOGY REVISIONS

[

]

With respect to the change control process resulting in the certification of UMAR16, AREVA's Software Quality Assurance Procedures for NRC approved methods require both the verification and validation (V&V) of code modifications and the assessment of the changes on the approved methodology results. These are two separate steps in the code release process.

1. The V&V of a code modification ensures the modification functions as intended. It includes new validation against data or higher order methods when the particular update modifies physical models and the existing test suite is inadequate to assess the change in performance.
2. In addition to the modification specific V&V described in item 1, AREVA evaluates the impact of the code modifications on the EM performance

through a series of tests referred to as the Continuity of Assessment (CoA) process. The CoA process recalculates a sufficient cross section of the analyses included in the methodology LTR to assess the impact of modifications relative to both the previous code version and to the final results (i.e. results updated as a result of RAIs) presented in the approved LTR.

[

]

**Table A.1 Identification of Modifications to ANP-10333P**

A large, empty rectangular frame with a thin black border, centered on the page. It appears to be a redaction of the table content mentioned in the caption above. The frame is oriented vertically and spans most of the width and height of the page's main content area.

## APPENDIX B

The sensitivity studies in Section 8.7.2 and 8.7.3 of the CRDA LTR have been evaluated with the enhanced convergence methodology which has been verified for the AURORA-B CRDA methodology. This enhanced convergence within the MB2-K module of S-RELAP5 has been verified for the AURORA-B AOO methodology. The sensitivity studies were repeated for Rod 118 and the results are provided in this appendix. As discussed in the RAI-4 and RAI-9 responses, the original conclusions drawn with the Rod 12 studies in the LTR remain appropriate.

### Initial coolant temperature 8.7.2.3:

The actual magnitude varies but the results show the similar trend as provided in Table 8.4 of the CRDA LTR.

**Table B.1 Core Initial Temperature Sensitivity Rod 118 EOFF**

### Initial Core Power Level Section 8.7.2.4:

The actual magnitude varies but the results show the similar trend as provided in Table 8.5 of the CRDA LTR. There are minor variations in the tail of the power pulse which results in slightly different values for total enthalpy when starting from a power level an order of magnitude greater.

**Table B.2 Core Initial Power Sensitivity Rod 118 EOFP**



Initial Core Flow Sensitivity Section 8.7.2.5:

In general the trend is similar to of Table 8.6 of the CRDA LTR, however the variation in the prompt enthalpy rise is small across the range of initial core flows with the latest code version. The total enthalpy trend is consistent and increases with core flow.

Examination of the tail of the power pulse shows that it [

] of rated flow for cold

startup conditions is appropriate.

**Table B.3 Core Initial Flow Sensitivity Rod 118 EOFP**



Fuel Rod Power History Section 8.7.2.6:

The fuel rod power history is addressed in RAI-3.

Moderator Feedback 8.7.3.2:

The actual magnitude of the impact varies for the moderator feedback however the results show the similar trend as provided in Table 8.12 and Table 8.13 of the CRDA LTR.

**Table B.4 Active Moderator Density Feedback**



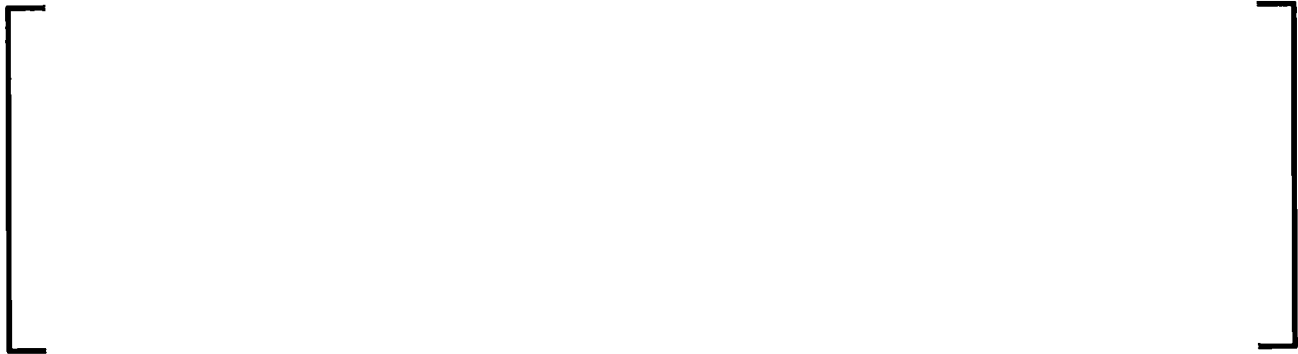
**Table B.5 Bypass Channel Moderator Density Feedback**



Fuel Temperature Feedback 8.7.3.2:

The results with the enhanced convergence are consistent with those given in Table 8.14 of the CRDA LTR.

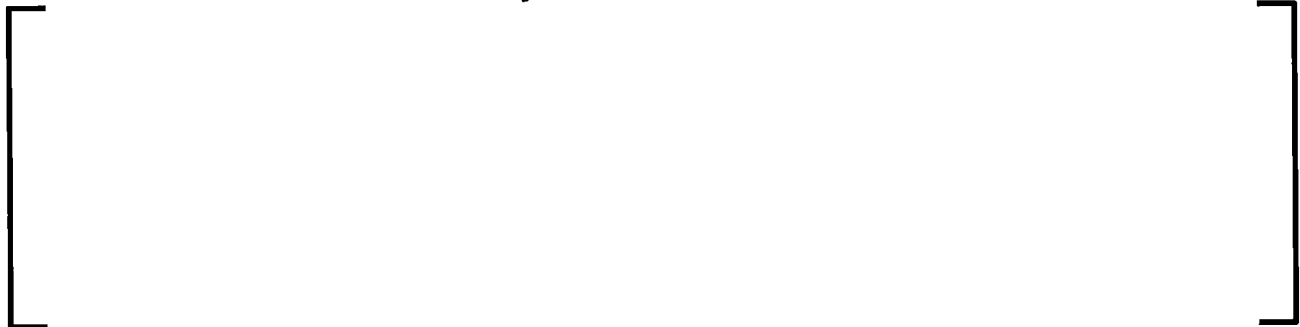
**Table B.6 Fuel Temperature Feedback**

A large pair of empty square brackets, one on the left and one on the right, spanning most of the page width. This indicates that the content of Table B.6 is missing from the document.

Effective Delayed-Neutron Fraction 8.7.3.2:

The results with the enhanced convergence are consistent with those given in Table 8.15 of the CRDA LTR. The conclusions in the CRDA LTR remain unchanged.

**Table B.7 Delayed Neutron Fraction Sensitivity**

A large pair of empty square brackets, one on the left and one on the right, spanning most of the page width. This indicates that the content of Table B.7 is missing from the document.

Heat Resistances in High Burnup Fuel, Gap, and Cladding 8.7.3.7:

The results with the enhanced convergence are consistent with those given in Tables 8.16 and 8.17 of the CRDA LTR. The conclusions in the CRDA LTR remain unchanged.

**Table B.8 Gap Width Adjustments**



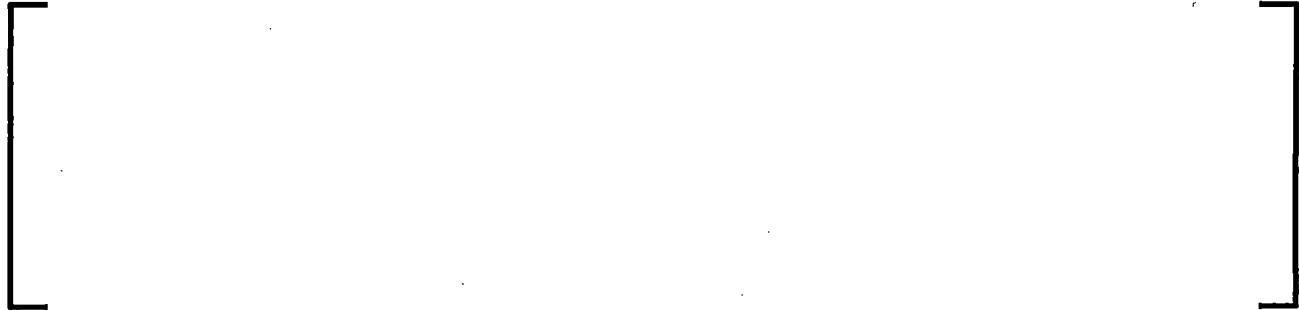
**Table B.9 Fuel Heat Transfer Coefficient Sensitivity**



Direct Energy Deposition to Moderator 8.7.3.10:

The results with the enhanced convergence are consistent with those given in Tables 8.18 of the CRDA LTR. The conclusions in the CRDA LTR remain unchanged.

**Table B.10 Heat Deposition Sensitivity**



Pellet Radial Power Distribution 8.7.3.11:

The results with the enhanced convergence are consistent for the prompt enthalpy rise with those given in Table 8.19 of the CRDA LTR. However, the total enthalpy rise values are larger. The selection of the Doppler weighting is discussed in detail in the response to RAI-1.

**Table B.11 Doppler Effective Temperature Coefficient Sensitivity**

